

ABSTRACT

In present paper, the LASCAD program was used to design and study the main important parameters that effect on diode pumped Nd:YAG disc laser, temperature distribution along the axis of laser disc and incident pump power . These influences on system performance were plotted and studied. "

KEYWORDS: high power, diode pumped laser, Nd:YAG laser, thin disk.

INTRODUCTION

Thermal lensing is of growing importance due to the tendency to miniaturize laser systems while simultaneously increasing their power output, causing 3D interaction of strong fields in tiny crystal volumes. The effect strongly depends on system characteristics such as material parameters, resonator geometry, pump beam distribution, and cooling layout. It interferes with gain guiding and other effects, which control beam quality and laser efficiency in a complicated manner. Based on a numerical simulation of these effects, LASCAD™ (**Laser Cavity Analysis and Design**) provides laser engineers with a quantitative understanding of the system characteristics prior to committing hard Finite Element Analysis (FEA) is used to compute temperature distribution, deformation, and stress or fracture mechanics in laser crystals, dependent on material properties, pump and cooling geometry. FEA is a well-known method to solve partial differential equations of technical physics such as the equation of conduction of heat numerically. Though indispensable and applied with great success in other engineering disciplines, it seems that the benefits of FEA for laser technology have not been fully recognized. In order to make this powerful analytical tool available for laser cavity design, LASCAD™ offers predesigned FEA models for important configurations such as end and side pumped rods, slabs, or thin disk lasers. Models are also available for crystals composed of various materials, or of doped and undoped regions, such as undoped end caps. The user can customize dimensions, FEA mesh, boundary conditions, and other parameters within the models. Temperature dependence of material parameters can be taken into account by the use of analytical expressions provided by the user. Analytical approximations based on super Gaussian functions are used to model pump light distribution. When using the FEA results with the ABCD matrix code the temperature distribution multiplied by the temperature dependence of the refractive index is fitted parabolically at right angles to the optical axis using the finite element mesh subdivisions. In the same way, a fit of the deformed end faces of the crystal is carried through. For many configurations - end pumped rods for example - this approximation is very close to reality, delivering reliable results for the laser mode. To visualize the results of the ABCD matrix code, the fundamental mode spot size as well as the phase front curvature along the resonator axis can be shown. End pumped bulk laser crystals are good candidates to high power and high beam quality lasers, but they are mainly limited by thermal effects. Thermal lensing, depolarisation losses and induced stress can lead to power losses, beam quality degradation or even fracture of the crystal^[1]. A better understanding of thermal issues is therefore needed to proceed to higher laser power. The most widespread way to investigate thermal effects in laser crystals is to use thermo-optical methods, that is thermal lens measurements or depolarization measurements. However, these methods only yield quantities that are proportional to thermal gradients inside the probed area, and they depend on the values of more or less known thermo-optical coefficients. Similarly, temperature distributions obtained by finite element analysis depend on material parameters which are not always well known or cannot be directly measured for instance the heat efficiency. Therefore, a direct method leading to absolute temperature mapping with high resolution is highly desirable^[2]. In this paper we present this kind of analysis for end-pumped configurations.

LASER DESIGN

Laser efficiencies

The relationship between the output power of the resonator and the pumping power is given by [2] .

$$P_{out} = P_p \eta_c \eta_a \eta_q \eta_s \eta_\varepsilon \eta_{out} \eta_m \quad (1)$$

Where P_p is the pump power, η_c is the coupling efficiency of the pumping system, η_a is the absorptivity of laser crystal to the pump light, η_q is the quantum efficiency of laser crystal (0.90 for Nd: AYG), η_s is stocks factor which is equal to the ratio of the pump wavelength to the laser wavelength (1.06 for Nd:YAG), η_ε is utilizing efficiency of the resonator's energy given by [2]

$$\eta_\varepsilon = 1 - \frac{P_{th}}{P_p} = 1 - \frac{g_{th}}{g_0} \quad (2)$$

With P_p : pump power, P_{th} : threshold pump power, g_0 small signal gain coefficient, g_{th} threshold small gain coefficient. η_{out} is the coupling efficiency of the output mirror given by [2]

$$\eta_{out} = -\ln \left[\frac{1}{M^2} \right] / -\ln \left[\frac{T^2}{M^2} \right] \quad (3)$$

M: magnification of the unstable cavity T: single transitivity of all optical elements in the cavity, $\eta_m = S_l/S_p$ is the utilizing efficiency of the mode volume with S_l : laser sectional area on disk, S_p : pump area on disk .
The laser should be designed to fulfill the maximum efficiency and perfect match of the every part .

Thermal Fracture Limits and Small Signal Gain Coefficient

The thickness of thin disk is determined by its thermal fracture limit. The maximum thermal power can endure for the thin disk cooled at one face is given by [1]

$$P_t = 6\gamma R_s \left[\frac{S}{t} \right] \quad (4)$$

Where R_s is the thermal impact parameter of Nd:YAG (11W/cm²), S is the area of the disk, t is the thickness of disk, γ is a constant related to the safety work of the laser, designed as 4.25, which means the laser working at the 15% fracture limit for full running^[3]. Therefore, the maximum absorbing power the disk permit is given by [1]

$$P_a = \frac{P_t}{\eta_n} \quad (5)$$

Where η_n is specific heat fraction per exited state (=0.32). The small signal gain coefficient of 1.7cm⁻¹ can be derived from relationship

$$g_0 = P_a / V I_s \quad (6)$$

Where V is the volume of the thin disk, I_s is the saturation intensity of Nd: YAG given by

$$I_s = h\nu / \sigma \tau_f \quad (7)$$

σ : emission section, τ_f : fluorescence lifetime, (h) Blank constant

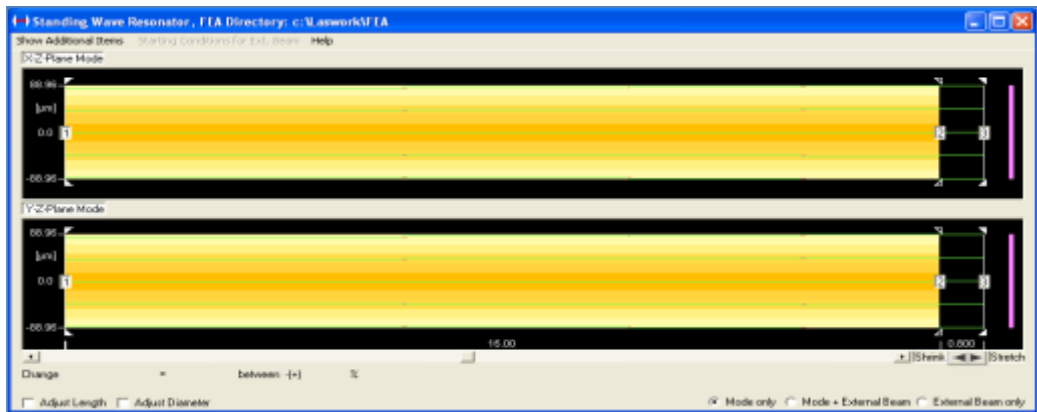
And with Lambert Law

$$I = I_0 \exp^{-\varepsilon c l} \quad (8)$$

Where I: is intensity, I_0 : is Intensity entering, ε :extinction coefficient, c : concentration of the solution , l : length of cavity .

LASCAD SIMULATION

Finite element analysis codes are a common way to investigate the thermal behavior of laser systems. However, the results of those simulations have not been checked so far by direct measurements. temperature mapping method enables us to do this verification, so compared experimental results with the FEA simulations of the LASCAD software^[4] (**Laser Cavity Analysis and Design**) for a Nd:YAG crystals

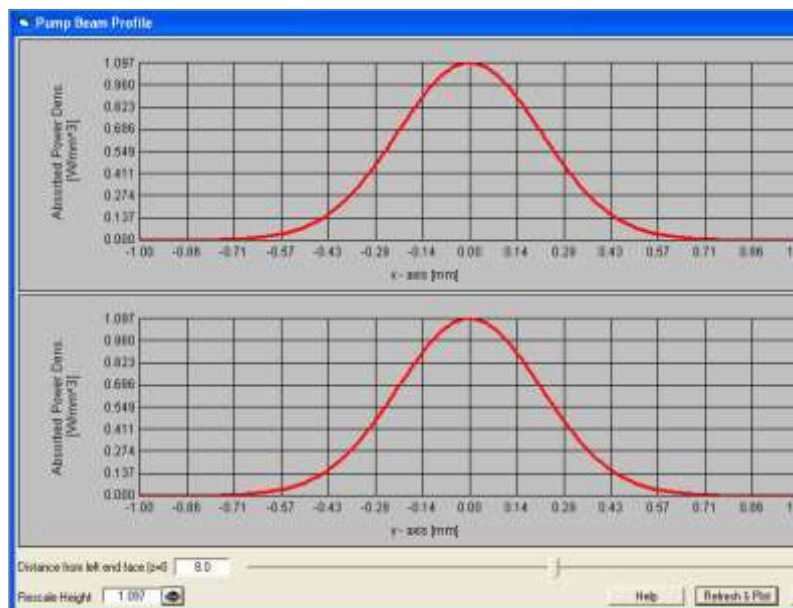


Fig(1) LASCAD program with Nd:YAG Crystal

Finite Element Analysis

To solve the differential equations for thermal and structural analysis (thermal deformation), applied a finite element discretization on semi-unstructured grids^{[5][6]} that have properties which are very useful in the application of laser simulation :

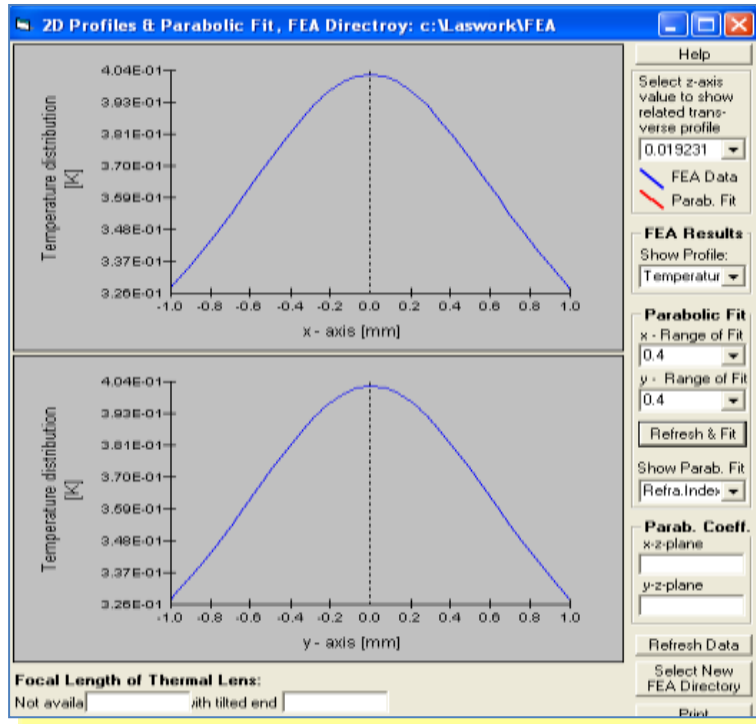
- Semi-unstructured grids calculate temperature distribution and deformation on a structured grid inside of the crystal which is very well suited for the analysis and interpolation of the data in a subsequent optical analysis of the cavity. This structured grid is connected to the surface of the crystal by small irregular elements.
- Semi-unstructured grids allow using fast computational codes. Different from irregular meshing computational time increases linearly with the number of grid points .
- Semi-unstructured grids can be stretched in x-, y-, and z-direction.
- High accuracy can be achieved by the use of small mesh size .
- The super-convergence of the gradient inside of the domain leads to an accurate approximation of the stress. In the present case, heat load distribution has been approximated by the use of super Gaussian functions in combination with an absorption coefficient. Boundary conditions have been defined by keeping the lateral surfaces of the crystal on constant temperature. Figure (2) shows the super gaussian function in combination with an absorption coefficient .



Fig(2) super gaussian function in combination with an absorption coefficient

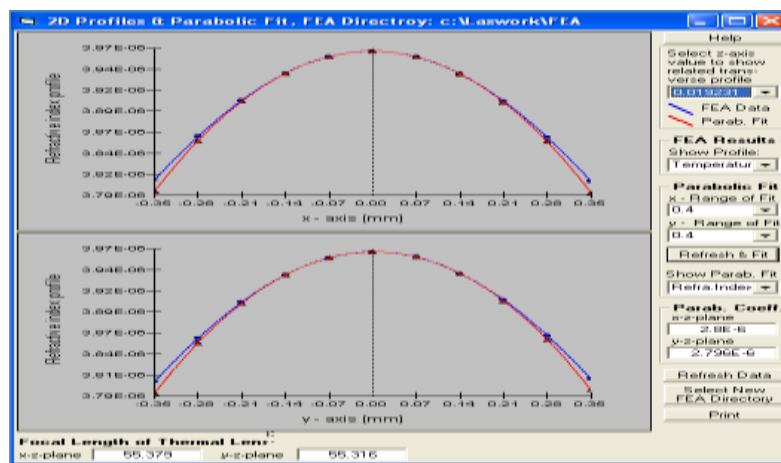
Measurements and Simulation

Alternatively it is possible to show 2D data profiles at different positions along the z-axis. The crystal was end-pumped by the laser diode at $\lambda = 0.810\mu\text{m}$. They were placed in parallel surface amount with fluid cooling system. The pump beam profile was Gaussian. The Nd:YAG crystal was 16 mm long, with a square cross section of 2mm. The incident pump beam was focused inside the crystal, at 1.00 mm of the entrance face. The diameter of the pump spot was $300\ \mu\text{m}$, with a divergence of 45 mrad. The incident power was 19.9W. The available positions correspond to the mesh subdivisions created by the FEA are plotted in figure (3).



Fig(3) The experimental and simulated temperature profiles

To fit the computed curves to the measured ones, a global heat efficiency factor has been used describing the fraction of pump power converted into heat. Obtained good agreement for a heat efficiency of 0.32 which is close to the commonly reported factor 0.32, see for instance [7]. With this parameter, the agreement between simulation and experiment is quite good, as the general shape and the temperature values are nearly the same. The non-symmetric shape of the experimental curve is due to a slight dissymmetry of the pumping configuration. Fig (4) shows fitting of simulated temperature profiles.



Fig(4) Fitting of simulated temperature profiles

We used a heat efficiency factor 0.32 to fit the curves, which is a bit higher than the factor 0.24 reported by Chen and Kuo[7] for lasing conditions. This deviation however may be explained by the fact that laser power extraction reduces the fraction of pump power converted into heat which is not the case in our experiments. The shape of those curves is quite different from those plotted for the Nd:YAG crystal because the pump spot is smaller. As a conclusion, the simulations were fitted with the experiments using reliable values for the heat efficiencies. The agreement observed validated our temperature mapping method.

Heat Transfer Measurements With Nd:YAG Crystal

One of the most important features of a solid-state laser system is the quality of the crystal cooling. To ensure a good heat removal, it's necessary that the heat transfer between the crystal and its mount is as good as possible. Measures of the heat transfer coefficient are usually difficult, but our thermal mapping method enables us to make it in a simple manner. The crystal used was 16 mm long, 2*2 mm² square cross section, It was placed in barrel surface amount with fluid cooling system. Figure(5) shows the temperature map obtained when the crystal is clamped by its four edge faces. In the first case, a clear gap is noticeable between the temperatures of the mount and at the edge of the crystal. The temperature distribution is parabolic inside the pumped region and then experiences a logarithmic decay until the edge of the crystal, in good agreement with the theory in the case of fiber-coupled diode pumping. The temperature difference at the center of the crystal between the two types of thermal contact shows clearly the importance of the interface.

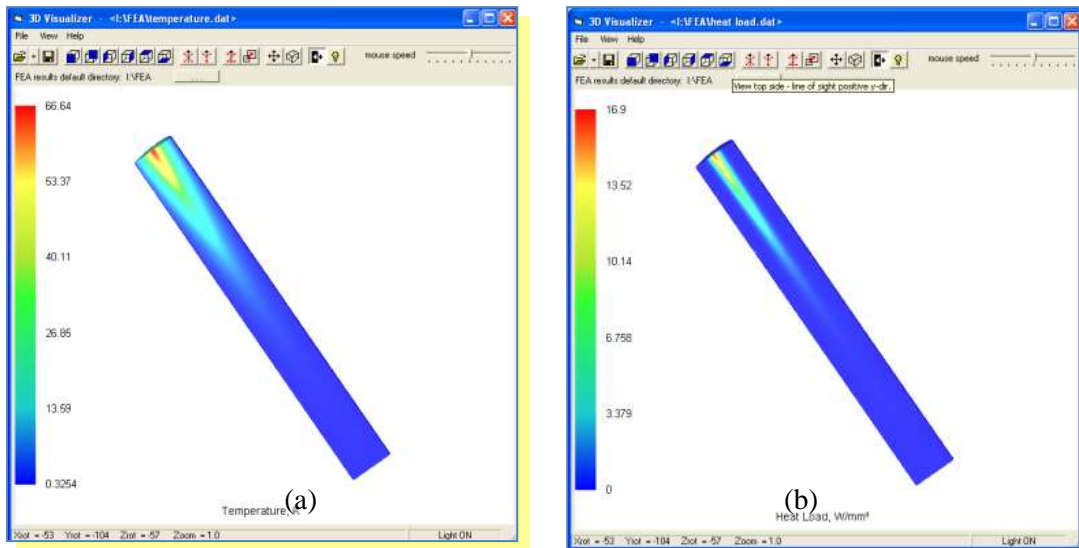


Fig (5) thermal mapping (a) temperature distribution (b) heat load distribution

Consequently studied more in details the heat contact. By analogy with convective transfer, the quality of the contact can be accounted by a heat transfer coefficient H (in W.cm-2.K-1), defined so that the heat flux through the surface is [2] :

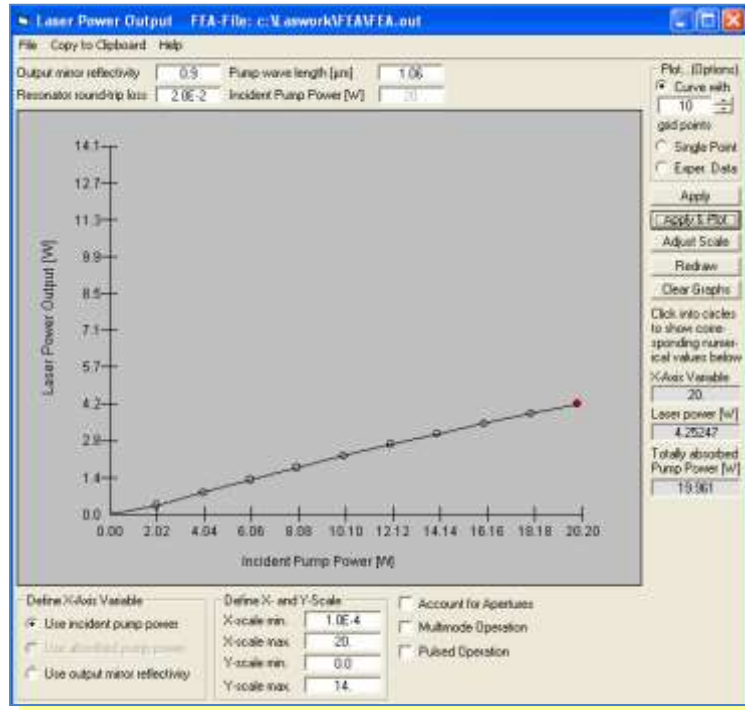
$$-K_c \|\vec{\nabla} T\|_e = H(T_e - T_m) \quad (9)$$

where K_c is the thermal conductivity of the crystal (W.cm-1.K-1), T_e the temperature at the edge of the crystal and T_m the heat sink temperature. The thermal gradient in(9) is considered normal to the surface. An ideal contact ($T_e=T_m$) corresponds to an infinite value of H. By performing a linear fit of the temperature versus position on the points that are closer to the crystal edge, the heat flux can be determined: by applying relation (9), one can then infer the value of H, which is here equal to 3.29 W.mm-2 in the case of bare contact. We estimate that the uncertainty on H is about 15%. The order of magnitude obtained is consistent with the values evoked by Carslaw3 and Koechner4. A hot spot can be noticed in figure 5.

Scaling output power

Scaling of output power is realized by increasing the pump diameter at a constant pump-power density on the disc and using several discs in series. In the design 10 discs is arranged along a folded unstable resonator axis because more 10 discs inside the resonator might be very difficult to align^[3] and a large laser beam diameter of 16mm is designed to fulfill the expected power of 19.9W. The laser power is 4.25W equal to laser transition saturation

intensity of Nd: YAG. The zigzag laser beam has an angle of 45° with the thin disk and an elliptical projective section on disk, so the pump area should also be ellipse for perfect match between the pump volume and the cavity mode. Figure (6) shows the relationship between laser output power and incident power .



Fig(6) Laser Power Output

CONCLUSION

In this paper we demonstrated the realization of a thermal mapping method of end-pumped laser crystals. We checked the validity of our calibration method, and the agreement between experiment and theoretical temperature maps at the crystal input surface were found to be very good in two different configurations. We have used our experimental setup to calculate by a simple method the heat transfer coefficient between a crystal and its mount

REFERENCES

- [1] Giesen, H. Hugel, A. Voss, et al., "Scalable Concept for Diode Pumped High Power Solid State Lasers", *Appl. Phys. B*, 58, 365-372, 1994 .
- [2] K. Contag, S. Erhasrd, A. Giesen, "Calculation of Optimum Design Parameters for Yb:YAG Thin Disk Lasers", *advanced solid laser*, 34, 124-130, 2000 .
- [3] H.Weber, "Diode Pumped Solid State lasers: From 10 W to 10 kW", *SPIE*. 3862, 2-10, 1999.
- [4] LASCADTM, <http://www.las-cad.com>.
- [5] Ch. Pflaum, "Semi-unstructured grids", *computing*, 67, 141 (2001).
- [6] K. Altmann, Ch. Pflaum, D. Seider, "Semi-unstructured grids in the laser simulation program LASCAD", *Proceeding of GAMM 2002* (2002).
- [7] T.Y. Fan, "Heat generation in Nd:YAG and Yb:YAG ", *IEEE J. of Q. El.*, 29, 1457 (1993).